THE ASTROPHYSICAL JOURNAL, 242:121–131, 1980 November 15

VELOCITY STRUCTURE IN THE CANIS MAJOR R1 MOLECULAR CLOUDS[1]

DENNIS E. MACHNIK, MICHAEL C. HETTRICK, AND MARC L. KUTNER
Physics Department, Rensselaer Polytechnic Institute
ROBERT L. DICKMAN
The Aerospace Corporation
AND
KENNETH D. TUCKER
Physics Department, Fordham University
Received 1980 March 31; accepted 1980 May 14

ABSTRACT

We have mapped CO emission over a $5° \times 5°$ area in the Canis Major OB1/R1 region. Most of the emission is confined to an elliptical region of approximately 90×60 pc. Several CO emission peaks appear, many associated with reflection nebulae. While most of the emission falls in the LSR velocity range 10–20 km s^{-1}, we find some material over the full velocity range covered (-30 to $+45$ km s^{-1}). There is no simple pattern that would indicate a single expanding shell, but the observations are consistent with the idea that some energetic process, which took place in an initially inhomogeneous cloudy medium, was responsible for the observed morphology of the region. Simple arguments suggest that a supernova explosion is the most likely candidate for this energetic process. The relationship between the process that shaped the clouds and star formation in the region is discussed.

Subject headings: clusters: associations — interstellar: molecules — nebulae: reflection — stars: formation

I. INTRODUCTION

Observations have firmly established a connection between OB associations and giant molecular clouds (e.g., Blitz 1978). However, the nature of the mechanism(s) that initiated star formation in these clouds is as yet unknown. Local mechanisms (in the sense that they operate over a scale the size of an association—tens of parsecs) recently proposed include the shock front preceding an ionization front from an H II region into a dense cloud (e.g., Elmegreen and Lada 1977), stellar winds (e.g., Blitz 1978), supernova blast waves (e.g., Herbst and Assousa 1977, 1978), and cloud-cloud collisions (e.g., Loren 1977).

In this paper we report observations of the molecular clouds in the vicinity of the OB association Canis Major OB1 and the R association (association of reflection nebulae, van den Bergh 1966) Canis Major R1 (Fig. 1). This region has been of considerable interest since the suggestion by Herbst and Assousa (1977) that it may have been a site of supernova-induced star formation. The arguments advanced by Herbst and Assousa are these: (1) CMa R1 is a site of recent star formation. It is claimed that the H-R diagram for the R association (Herbst, Racine, and Warner 1978) suggests an age of about 3×10^5 yr. (2) A well-defined arc or ring structure in Hα surrounds the region, suggesting a previous central energetic process. In addition, it is argued that there is evidence for an expanding gas shell, both in the 21 cm observations of Weaver and Williams (1974) and in the splitting of the [N II] line observed by Reynolds and Ogden (1978). Herbst and Assousa (1977) infer an H I expansion velocity of 32 km s^{-1}, while the [N II] observations suggest an expansion velocity of 13 km s^{-1}. (3) In an OB association of the age estimated for CMa OB1, it would appear reasonable that one or more massive stars has had sufficient time to evolve into a supernova. Indeed, one member of the association is identified as a runaway star. (4) The distribution of young stars in the region, with most confined to a small arc on the western edge of the ring, suggests a causal relationship between the postulated supernova and the formation of these stars.

Several arguments have been raised against the above picture (e.g., Lada, Blitz, and Elmegreen 1978). (1) Some doubt exists regarding the reality of the expanding H I feature. Moreover, if the H I shell is real, the discrepancy between the expansion velocity obtained from the 21 cm observations and that obtained from the [N II] observations must be explained. (2) There are

[1]This research was partially supported by the Aerospace Corporate Programs for Research and Investigation.

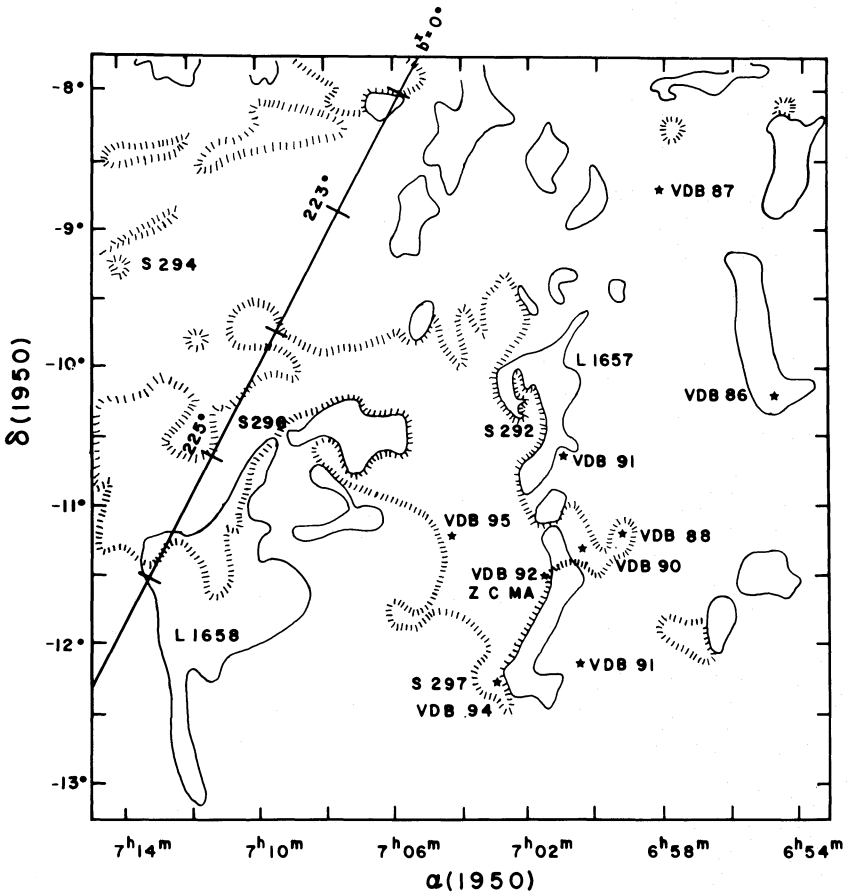

FIG. 1.—A sketch of the CMa OB1/R1 region, made from the Palomar Sky Survey red and blue prints. Solid lines indicate the approximate boundaries of dark clouds. Hatched boundaries surround emission nebulosities. Stars mark the position of reflection nebulae and the "VDB" numbers refer to the catalog of van den Bergh (1966).

problems with the time scales involved. It is not clear that the age of the R association is sufficiently less than the expansion time of the shell for a causal relationship to exist.

These objections make it clear that three essentially independent issues must be addressed in order to clarify the evolutionary status of the CMa OB1/R1 region: (*a*) Was a past energetic process (either gradual or explosive) responsible for the observed morphology of the interstellar material? (*b*) Was that process the passage of a supernova blast wave? (*c*) Independent of the nature of the process, what is its relationship to star formation in the region?

II. OBSERVATIONS

Most of the observations reported here were made with the 4.6 m telescope of the Aerospace Corporation, El Segundo, California. At 2.6 mm, the half-power beam width (HPBW) was 2'.6 (corresponding to about 0.9 pc at the adopted distance of 1100 pc to the OB association). A velocity resolution of 0.65 km s^{-1} was used, and all spectra covered an LSR velocity range of -30 to $+45$ km s^{-1}. This large velocity coverage was important in view of the possibility of extreme-velocity material from some energetic process. Spectra were taken with frequency switching by an amount small compared with the total bandwidth. This procedure was satisfactory, since even though lines were detected over a large velocity range, they appeared as individual narrow features, rather than as a single broad line. Positions for which the particular switching appeared to cause ambiguities were reobserved with an appropriate switching. Off-source spectra were subtracted from on-source spectra. Calibration was done using a chopper wheel at ambient temperature, with corrections for atmospheric attenuation carried out as described by Kutner (1978). All line temperatures quoted here are radiation temperatures, T_R, corrected for atmospheric absorption and beam efficiency. On this scale, the radiation temperature of the CO line in the direction of the Kleinmann-Low nebula in Orion is 65 K.

Some supplementary observations were obtained with the 11 m telescope of the National Radio Astronomy

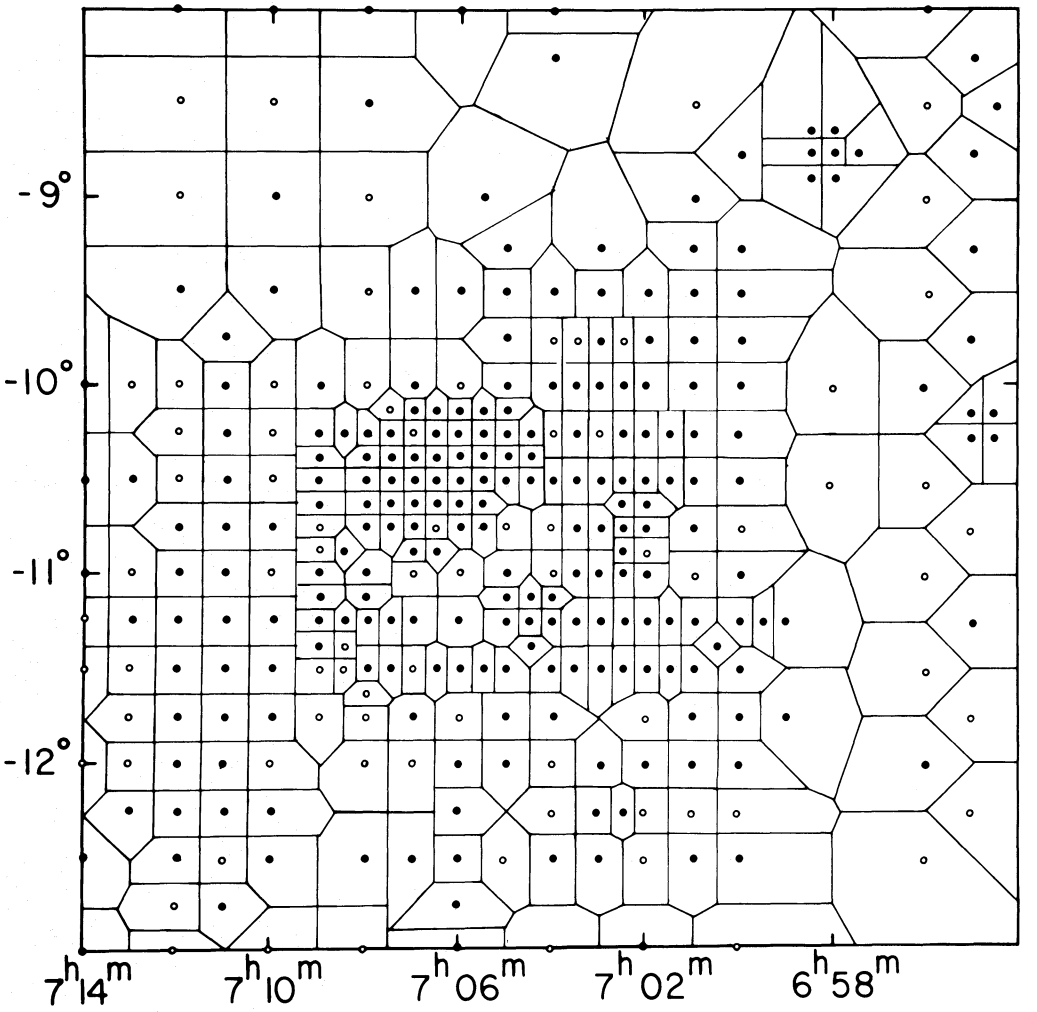

FIG. 2.—Positions of CO observations. Filled circles represent CO detections, and open circles represent negative results. The solid lines around each circle surround those plotting array points for which the given circle is the closest data point.

Observatory,[2] located on Kitt Peak. The HPBW was 70″, and a velocity resolution of 0.65 km s^{-1} was used. Observations were made while switching once per minute between the source position and a reference position. Calibration was done as above, and the CO radiation temperature in the direction of the KL nebula was 70 K. For the most part, the 11 m telescope was used for higher-resolution mapping around selected reflection nebulae (Kutner *et al.* 1980).

Our map covers the 315 positions shown in Figure 2, with a typical rms noise level of 0.5 K. Filled circles represent the 236 positions where CO was detected, and the open circles represent the 79 positions where CO was not detected. The typical separation between observed points was 7.5 (approximately 2.6 pc), and the area covered by the observations is about 5° × 5°.

The results of the observations are presented in the next section (§ III), and many of these results are in the form of contour maps. Since the data do not completely sample the region and also sample at irregular intervals, it is important to know how these maps were constructed, so that the contours can be properly interpreted. The actual spectra formed an inappropriate basis for a contour mapping program because of the presence of frequency-switching images and large-scale baseline curvature. However, baseline curvature did not affect the determination of any line parameters since the observed lines were at most a few km s^{-1} wide. Therefore, Gaussians were fitted to each spectral line observed, and, for the purposes of plotting, the spectrum at each position was taken as the sum of all

[2]The National Radio Astronomy Observatory is operated by Associated Universities, Inc., under contract with the National Science Foundation.

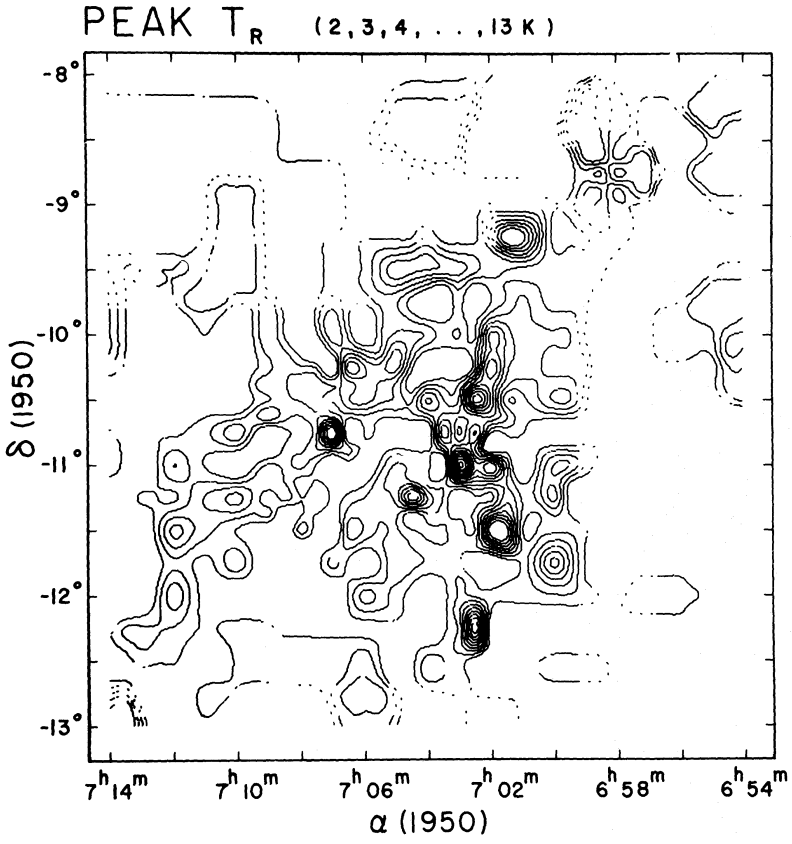

FIG. 3*a*

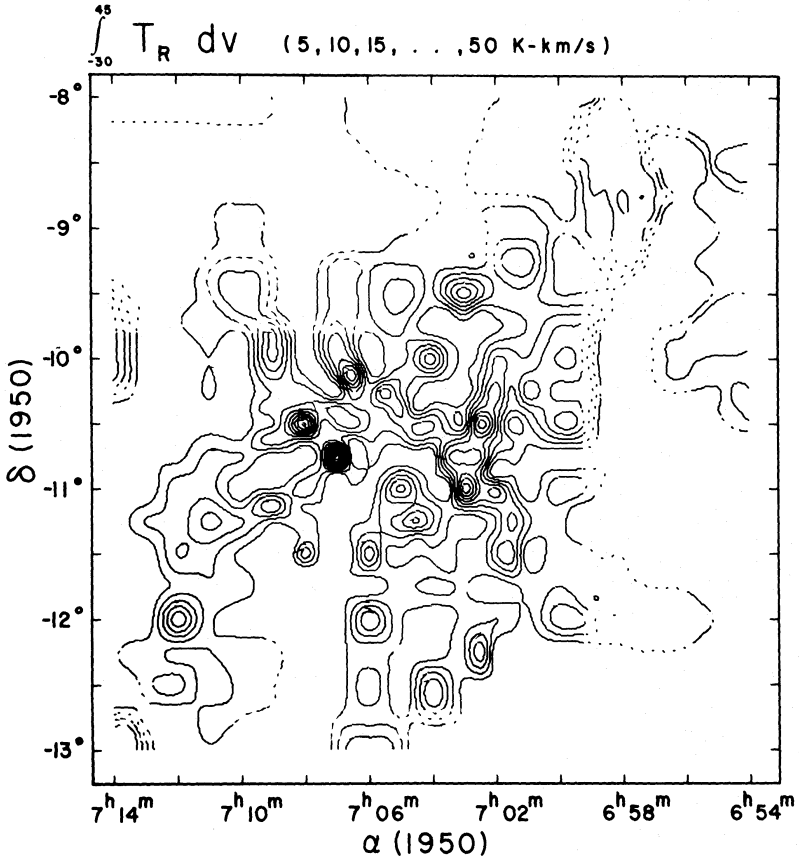

FIG. 3*b*

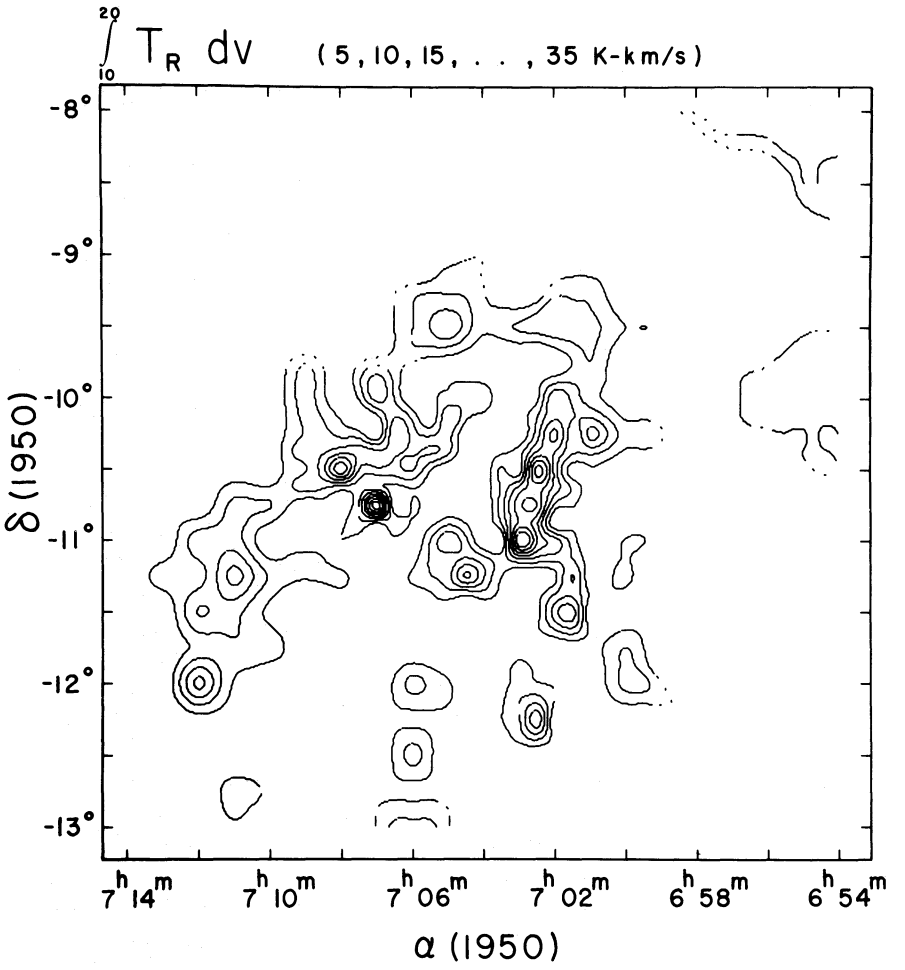

FIG. 3c

FIG. 3.—The CO distribution in CMa. (*a*) Contours of equal peak-line radiation temperature with contour levels as indicated above the map. Dashed lines indicate no data points within 10′. (*b*) Contours of equal integrated radiation temperature with the velocity integration being carried out over the full velocity range of the survey. In comparing this map with those of Blitz (1978), note that Blitz's line temperatures are in T_A^*, uncorrected for beam efficiency. (*c*) Contours of equal integrated T_R with the velocity integration carried out from 10 to 20 km s^{-1}, the range where most of the material is found.

the Gaussians needed to reproduce the lines at that position. These composite spectra produced good reproductions of the lines to within the noise level. (Since the contour maps which follow were constructed from these composite spectra, every feature corresponds to a line whose reality was verified by inspection of the original spectra. This procedure, however, is insensitive to spatially extended but low-level features, whose reality would otherwise be enhanced by their appearance in several adjacent spectra.) Contour maps were generated from a 41×41 point plotting array, corresponding to a 7.5 spacing. Where incomplete sampling occurred (especially near the edges), the value at a given array point is taken to be the value at the nearest observed point. Contours were generated as bicubic splines. In each of the contour maps, dashed lines indicate no data point within 10′.

III. RESULTS

The overall distribution of CO in this region is shown in Figure 3, in three different representations. The first two show contours of peak T_R and $\int T_R dv$ from −30 to +45 km s^{-1}. The third plot shows $\int T_R dv$ from 10 to 20 km s^{-1}; since, as will be discussed below, most of the material appears in this velocity range, one can thus see major structures with a minimum of confusion from foreground and background material. We note also that 15 km s^{-1} is the LSR velocity expected for this region on the basis of simple differential galactic rotation.

TABLE 1

CO PEAKS IN CANIS MAJOR R1

α(1950)	δ(1950)	Type[a]	Notes
$6^h59^m05^s$ ...	−8°38′	*T*	
6 59 37 ...	−12 04	*T*, *I*	Extended peak near VDB 89
7 01 10 ...	−9 19	*T*	Blitz peak J
7 01 45 ...	−11 33	*T*, *I*	Near VDB 92 and Z CMa
7 02 30 ...	−10 31	*T*, *I*	S292, Blitz peak C
7 02 31 ...	−12 17	*T*, *I*	VDB 94
7 02 55 ...	−11 02	*T*, *I*	Blitz peak B
7 03 02 ...	−9 33	*I*	
7 04 00 ...	−12 41	*I*	
7 04 02 ...	−10 03	*I*	Near NGC 2335
7 04 26 ...	−9 34	*T*	
7 04 35 ...	−11 14	*T*, *I*	VDB 95
7 05 02 ...	−11 01	*I*	
7 05 33 ...	−10 15	*I*	
7 05 59 ...	−12 04	*I*	
7 06 01 ...	−11 33	*I*	
7 06 35 ...	−10 07	*I*	Blitz peak E
7 07 02 ...	−10 44	*T*, *I*	
7 08 08 ...	−10 30	*I*	Blitz peak D
7 09 05 ...	−10 03	*I*	Blitz peak M
7 09 09 ...	−11 09	*I*	
7 10 54 ...	−11 19	*I*	Blitz peaks K, L
7 12 00 ...	−12 04	*T*, *I*	

[a] *T* indicates peak in T_R map; *I* indicates peak in $\int T_R dv$ map.

Most of the CO emission is confined within an ellipse centered near $7^h\ 06\overset{m}{.}0$, −11°, with dimensions of about 4°.5×3° (90×60 pc). Within this boundary the distribution of material might be described as two contiguous annuli (a figure eight). The larger annulus is centered near $7^h\ 06\overset{m}{.}5$, −11° 45′, with a diameter of about 3° (60 pc) and thickness of about 0°.8 (14 pc); and the smaller one is centered near $7^h\ 03\overset{m}{.}0$, −10°, with a diameter of about 1° (20 pc) and a thickness comparable to that of the larger annulus.

A CO map of this region, with 10′ angular resolution and 2.6 km s^{-1} velocity resolution covering only positive LSR velocities has been made by Blitz (1978). In comparing our results with those of Blitz, we find that, to within the limits of both surveys, they are in agreement. With our slightly better sensitivity and greater velocity range, we find more emission in the central region of the cloud complex.

Our maps show about 20 spatial peaks in CO emission, listed in Table 1. Four of these appear to be associated with reflection nebulae (numbers 89, 92, 94, and 95 in the catalog of van den Bergh 1966 [VDB]). For more detailed information on VDB 92 (which also includes Z CMa), 94, and 95, see Kutner *et al.* (1980). The material associated with VDB 95 appears to fill part of the interior of the ring and lies at a velocity of about 15 km s^{-1}. Five of the CO peaks (including one associated with S292, as well as those associated with VDB 92 and 94) appear to lie along the edge of emission nebulosity and narrow dark cloud on the west side of the ring and coincide with the region proposed by Herbst and Assousa (1978) as one of the sites of recent star formation. Herbst, Racine, and Warner (1978) have found several faint reflection nebulae along this cloud, and further high-resolution molecular observations will be necessary to see how closely the CO peaks correspond to these reflection nebulae.

The velocity structure of the molecular material is displayed in Figures 4–7. In Figure 4 we present a sum

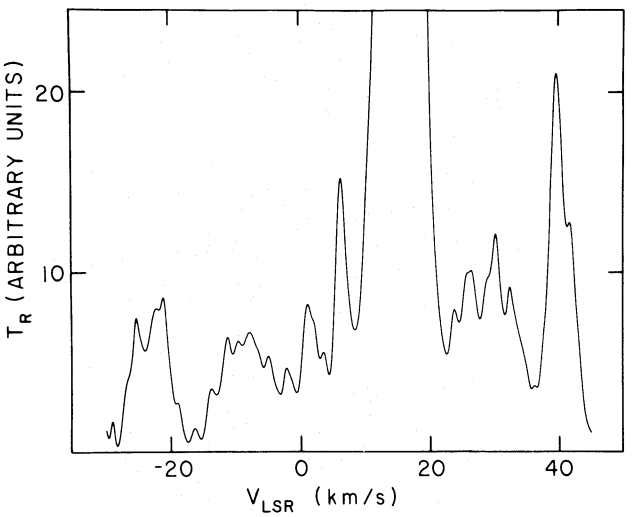

FIG. 4.—A composite of all the observed line profiles. The units are arbitrary with the strongest peak being 100 units high. No correction has been made for the irregular sampling.

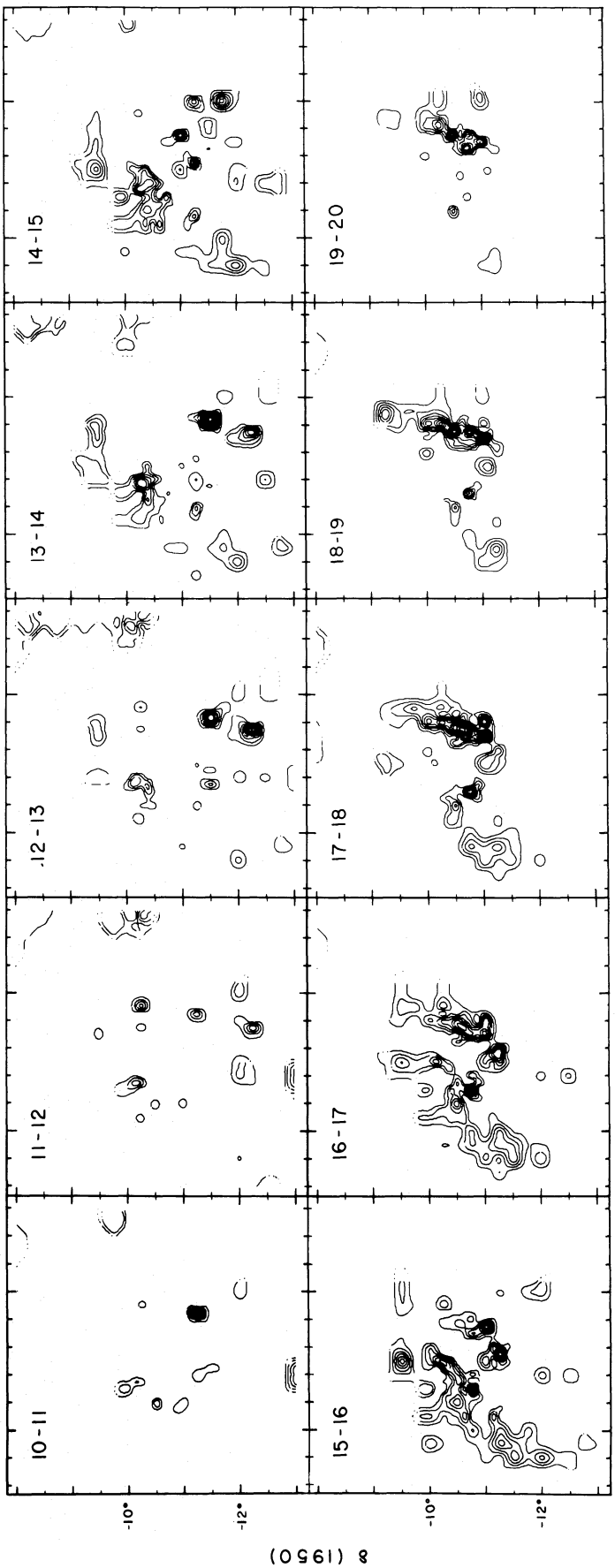

FIG. 5.—Contours of equal integrated intensity in 1 km s^{-1} steps over the 10–20 km s^{-1} range. Contour levels are as in Fig. 3*c*.

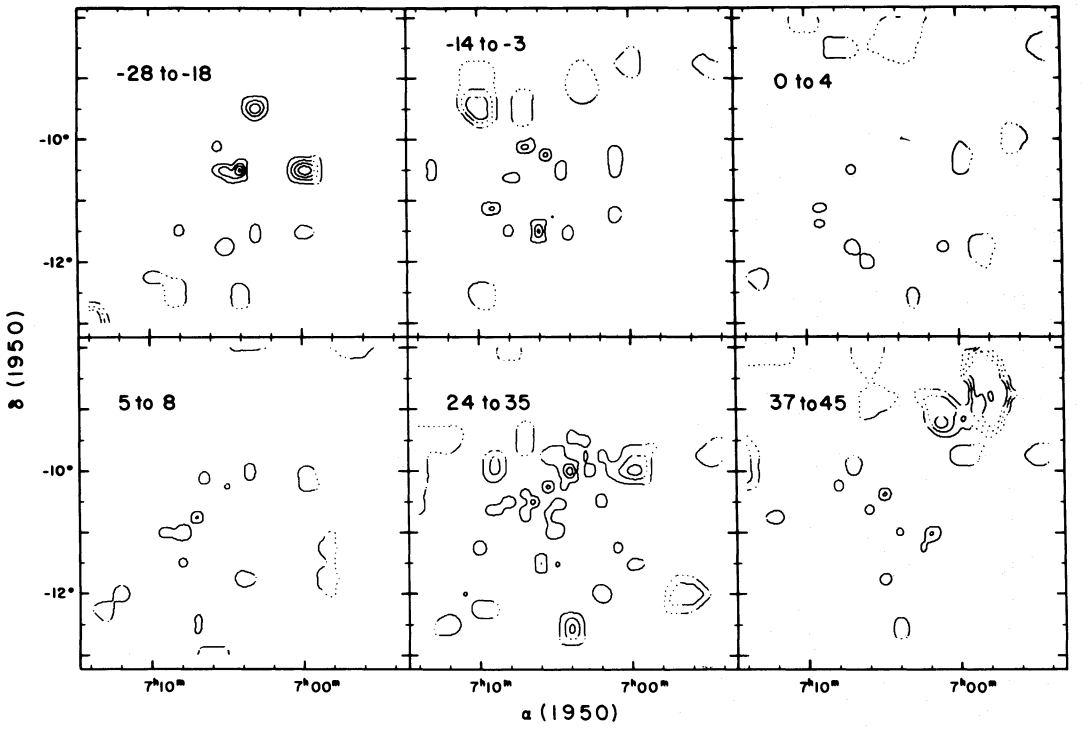

FIG. 6.—Contours of equal integrated intensity with the ranges of integration corresponding to the velocity ranges of the various features in Fig. 4. Contour levels are as in Fig. 3*c*.

of the Gaussian profiles from all 315 CO spectra. While absolute and exact relative intensities in this spectrum are not meaningful, specific velocity features can be seen. Most of the emission lies in the range 10–20 km s^{-1}, but emission is observed over the full range from -30 to $+45$ km s^{-1}.

To study the 10–20 km s^{-1} material in some detail, Figure 5 gives the $\int T_R dv$ in 1 km s^{-1} steps. The two-cloud structure pointed out by Blitz (1978) is evident. The cloud L 1658 (S296) predominates at 15–16 km s^{-1} and appears in the eastern and northwestern part of the ring. At 14 km s^{-1} this cloud separates into a northern and southern part. The S292 cloud predominates at 17–18 km s^{-1} and appears in the western part of the ring. Two peaks in the southwest part of the ring show up best at 13 km s^{-1}. Most of the material below a declination of $-12°$ is in the 10–15 km s^{-1} range. Coordinate-velocity maps reveal what may be an average velocity gradient of 0.1 km s^{-1} pc^{-1}, which shows up best perpendicular to the galactic plane (see below and Fig. 7).

The large-scale velocity structure is illustrated in Figure 6, in which $\int T_R dv$ is shown integrated over ranges corresponding to the features identified in Figure 4. One striking feature of these maps is the presence of material with $v(\mathrm{LSR}) < 0$ in a region of the galaxy for which differential rotation should produce only positive velocities. This negative-velocity material appears in small clumps and in no persistent pattern (although within each figure there is a suggestion of a ring pattern). Some recent observations made on the 11 m telescope, and not included in the maps, suggest that some of the individual negative-velocity clumps may be smaller than suggested by our sparsely sampled contour map. There is also material at positive velocities well beyond those expected for the CMa region. This could, of course, be due to background material, for which such velocities are allowed by the normal differential rotation. A different view of the distribution of the most negative- and positive-velocity material can be obtained from Figure 7, which presents the data in the form of l^{II}-v and b^{II}-v maps. The material shows some confinement to the range $223°.3 < l^{II} < 225°.5$, and $-2°.5 < b^{II} < 0°$. These distributions will be discussed in the next section (§ IV).

IV. DISCUSSION

a) *An Energetic Process*?

An expanding shell is the simplest configuration one could expect for an ensemble of molecular clouds whose morphology has been ordered by a central energetic process. However, if the CMa OB1 molecular clouds are indeed part of an expanding shell, one would expect a systematic change in the size of a ring as one looks at different radial velocity material. A look at

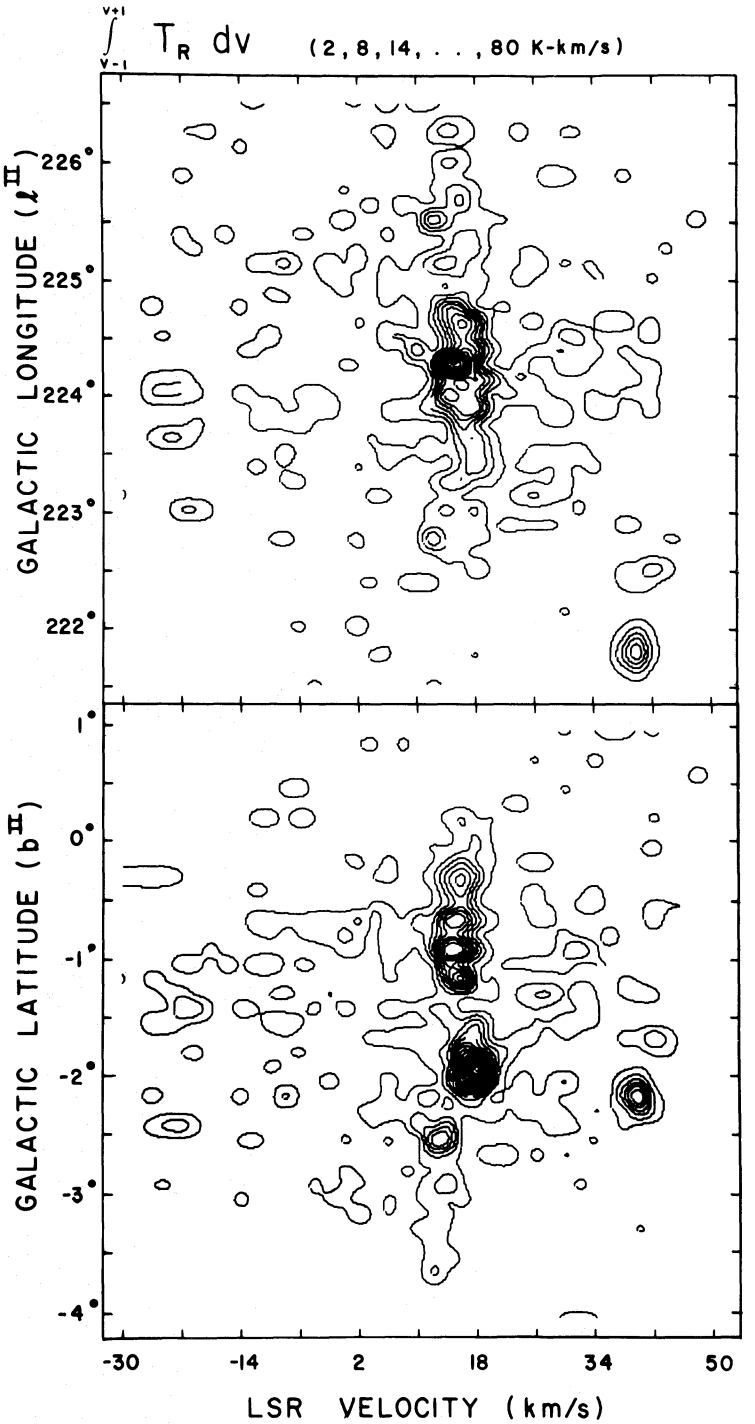

FIG. 7.—Contours of equal integrated intensity in coordinate-velocity representation. The velocity integration is in 2 km s^{-1} steps. In the upper map, data at a given longitude is the sum of spectra at all points at that longitude. Similarly, in the lower map, data at a given latitude is the sum of spectra at all points at that latitude.

Figure 6 (with Fig. 3*c* inserted in proper sequence) shows no simple pattern. It might be that such a pattern is present, but the clumpiness of the material hides it from the eye. However, one can get a more unbiased view by plotting (for several velocity ranges) the integrated intensity in annuli of different radii and looking for systematic size changes. We have done this for circles with different centers and for ellipses with

different centers, orientations, and eccentricities. In all of these, no systematic pattern of size versus velocity emerges. From this we conclude that there is no evidence for a simple expanding molecular shell.

However, the above discussion does not rule out the possibility that an energetic process played an important role in shaping the observed cloud structure. In particular, there is the negative-velocity material, well outside the allowed velocity range for this part of the galaxy. With respect to the 15 km s^{-1} mean velocity for this region, the -30 km s^{-1} material has a velocity of 45 km s^{-1}. If this material is associated with the CMa R1 molecular clouds, the velocity difference suggests some energetic process. The same might be said for the material observed between 20 and 45 km s^{-1}.

Is the negative-velocity material associated with the CMa R1 molecular clouds? While it would be easier to tell if our map covered a much larger cale, and we definitely saw no such material elsewhere in this part of the galaxy, there is still some information in the present data. From Figure 6, it is seen that the bulk of the -28 to -18, and -14 to -3 km s^{-1} material has a distribution similar to that at 0 to 4, 5 to 8, or 10 to 20 km s^{-1}. Figure 7 shows some information in the distribution of the negative-velocity material in l^{II} and b^{II}. In l^{II}, though a more extended sample would make the case stronger, it appears that most of the $v(\mathrm{LSR})<0$ material is confined between 223° and 225°.5, with the extreme velocity coming at about 224°. In b^{II}, most of this material is confined to $-2°.5<b^{II}<0°$, with a center at $-1°.5$ (not 0° as might be expected for more generally distributed material). We conclude from this that the distribution of the negative-velocity material in CMa is similar to that of the 10–20 km s^{-1} material and that an association of the material with the CMa R1 molecular complex is likely. Of course, more extensive observations will be required to establish this more firmly.

The same morphological arguments can be made for the $v(\mathrm{LSR})>20$ km s^{-1} material, based on Figures 6 and 7. Such arguments are necessarily weaker, given that background sources at allowed galactic rotation speeds can contaminate CO emission at positive v(LSR). However, pending further observations, we tentatively conclude that much of the material falling outside the 10–20 km s^{-1} range is still associated with the CMa R1 region. For simplicity, in the remainder of the discussion, we will refer to the clouds with $v(\mathrm{LSR})<0$ and $v(\mathrm{LSR})>20$ km s^{-1}, as the "extreme velocity" material.

The existence of extreme-velocity material would suggest some energetic process. However, one must then explain the absence of an essentially hollow expanding shell and also explain the differences between the extreme CO velocities and the 35 km s^{-1} derived from the 21 cm observations or the 13 km s^{-1} derived from the [N II] observations. Several factors could inhibit the development of a simple expanding shell concentric with the source of the energetic process. First, given the observational fact that H II regions tend to occur at the edges of massive clouds, central symmetry would evidently be unlikely. Second, hydrodynamic (e.g., Rayleigh-Taylor) instabilities will, to some extent, destroy the coherence of an expanding shell. Finally, the fact that *complexes* of molecular clouds are associated with H II regions makes it necessary to consider the response of an initially dense and inhomogeneous medium to the processes under discussion here. This point has already been raised by Kutner *et al.* (1979) in connection with CO observations of the Mon R1 molecular clouds.

The notion of an initially inhomogeneous medium is consistent with the observation that the extreme-velocity material is essentially fragmentary. If we consider an initial distribution of clouds of comparable density but different size, any accelerating force should vary as L^2, where L is a typical length scale of a cloud fragment, while the mass varies as L^3; the acceleration of a fragment should hence vary as $1/L$. Smaller fragments would then attain higher velocities, explaining the spread in velocities and the fact that no simple velocity pattern emerges from our data. (Note that if the larger clumps have higher density than the smaller clumps, the velocity difference is even more pronounced.) Any attempt to reasonably fit 21 cm observations into this picture must await new observations done with better resolution and sensitivity than the Weaver and Williams (1974) survey. Higher resolution would make it easier to trace out the velocity structure of any possible H I ring and would minimize the amount of foreground and background material in any line of sight. Greater sensitivity would allow one to determine if there are any H I clumps at high velocities, corresponding to molecular fragments.

The detailed velocity structure of the 10–20 km s^{-1} material might be fitted into this picture, if we interpret the velocity difference between the eastern and western clouds as being a projection of the expansion. The small velocity difference, about 3 km s^{-1}, is not unreasonable for two reasons: (1) These larger clouds will not have velocities comparable to the small fragments, and, based on the size contrast, a velocity difference of less than 10 km s^{-1} might be expected. (2) It is unlikely that the expansion of the large clouds is being viewed edge-on, so there is some projection effect. (A similar behavior is observed in the Mon R1 clouds, where opposite sides of a ring have velocities that differ by 3 km s^{-1}.) Whether or not the velocity difference between the large clouds can be explained in this manner, it seems that the CO data do support the idea of an energetic process being responsible for shaping the present cloud structure.

b) A Supernova?

Since our data suggest an energetic process as being responsible for the structure of the CMa clouds, we also ask if the data can help to establish the nature of this process. An extension of the simple model discussed above, in which smaller clouds have greater velocities, provides some information. From a dynamical standpoint, the basic difference between a supernova and either an expanding H II region or a stellar wind is that the supernova produces the acceleration of the clouds in a time short compared with the expansion age, whereas the others produce more gradual accelerations over a longer time. Under a gradual acceleration, smaller clouds still acquire larger velocities. However, as such small clouds move out ahead of larger ones, their acceleration drops off as $1/r^2$, where r is the distance from the center of expansion. This tends to reduce the velocity contrast between the smaller and larger clouds. Thus, a gradual process is more likely to build up a well-defined shell, an effect which would be enhanced by any braking effect of the ambient medium.

A very simple analysis suggests that after 10^6 yr, velocities will scale as $1/L^{1/2}$ for a gradual process and as $1/L$ for an explosive process. It would thus seem that the large velocity spread and irregular spatial distribution, especially the absence of a hollow shell, are more consistent with an explosive, rather than gradual, expansion.

Of course, this conclusion must be regarded as tentative for at least two reasons: (1) We are making dynamical arguments without a real knowledge of the masses involved. Mass estimates will require extensive ^{13}CO observations. (2) No detailed hydrodynamic calculations have been made to support the crude calculations mentioned above, though Woodward (1978) has modeled CMa R1 with a supernova explosion in a dense cloud. In particular, it will be necessary to investigate the dependence of velocity on initial cloud size for the various processes suggested.

c) Relation to Star Formation

One objection to the R association having been formed by a supernova in the OB association is based on time scales. In particular, Blitz (1978) has argued that the free-fall collapse time of the molecular clouds may be comparable to the expansion age of the region, allowing insufficient time for star formation. However, if the expansion started in a medium already populated by molecular clouds, with a clumpy distribution, this time scale is somewhat reduced. (At a molecular hydrogen density of 10^4 cm^{-3}, the free-fall time is 4×10^5 yr.) In addition, any such estimate must utilize the postshock density, which will be somewhat higher than the average molecular cloud density. Thus, there may have been sufficient time for star formation.

Whatever the cause, if an expansion was initiated 10^6 yr ago, this may have initiated star formation in the molecular clouds. Since the estimated expansion age is comparable to the free-fall time, evidence of that star formation may just now be appearing. The signposts of such formation may be the CO hot spots that show up on our map but are not obviously associated with any optical object. Further investigation on this possibility will have to await much more detailed CO and ^{13}CO observations, especially on the western side of the observed ring.

M. L. K. would like to acknowledge partial support from National Science Foundation grant AST76-17834 and a grant from the Research Corporation. K. D. T. acknowledges support from the Research Corporation and a Fordham University faculty research grant. M. C. H. was partially supported by NSF grant SPI77-26207. R. L. D.'s work was partially supported by the Aerospace Corporate Programs for Research and Investigation. The millimeter observations at the Aerospace Corporation were partially supported by NSF grant MPS73-04554 and the Aerospace Corporate Programs for Research and Investigation.

REFERENCES

Blitz, L. 1978, Ph.D. thesis, Columbia University.
Elmegreen, B., and Lada, C. J. 1977, *Ap. J.*, **214**, 725.
Herbst, W., and Assousa, G. E. 1977, *Ap. J.*, **217**, 473.
_____. 1978, in *Protostars and Planets*, ed. T. Gerhrels (Tucson: University of Arizona Press), p. 368.
Herbst, W., Racine, R., and Warner, J. W. 1978, *Ap. J.*, **223**, 471.
Kutner, M. L. 1978, *Ap. Letters*, **19**, 81.
Kutner, M. L., Dickman, R. L., Tucker, K. D., and Machnik, D. E. 1979, *Ap. J.*, **232**, 724.
Kutner, M. L., Machnik, D. E., Tucker, K. D., and Dickman, R. L. 1980, *Ap. J.*, **237**, 734.
Lada, C. J., Blitz, L., and Elmegreen, B. G. 1978, in *Protostars and Planets*, ed. T. Gehrels (Tucson: University of Arizona Press), p. 341.
Loren, R. 1977, *Ap. J.*, **215**, 129.
Reynolds, R. J., and Ogden, P. M. 1978, *Ap. J.*, **224**, 94.
van den Bergh, S. 1966, *A. J.*, **71**, 990.
Weaver, H., and Williams, D. R. W. 1974, *Astr. Ap. Suppl.*, **17**, 1.
Woodward, P. R. 1978, *Proc. Internat. School of Physics, Enrico Fermi*, course No. 73.

R. L. DICKMAN: F.C.R.A.O., University of Massachusetts, Amherst, MA 01003

M. C. HETTRICK: Department of Astronomy, University of California, Berkeley, CA 94720

M. L. KUTNER and D. E. MACHNIK: Physics Department, Rensselaer Polytechnic Institute, Troy, NY 12181

K. D. TUCKER: Physics Department, Fordham University, Bronx, NY 10458